

Anderson phases as precursors of nickel–molybdenum–tungsten oxides

Piero Porta,^{*a} Giuliano Minelli,^a Ida Pettiti,^a Lia I. Botto^b and Horacio J. Thomas^b

^aCentro del Consiglio Nazionale delle Ricerche su 'Struttura ed Attività Catalitica di Sistemi di Ossidi' (SACSO), c/o Dipartimento di Chimica Università 'La Sapienza', Piazzale Aldo Moro 5, 00185 Roma, Italy

^bQuímica Inorgánica and CINDECA-CONICET, Facultad de Ciencias Exactas, Universidad Nacional de La Plata, 1900-La Plata, Argentina

Mixed Ni–Mo–W oxides have been prepared by decomposition at 873 K of Anderson-type $[\text{NiMo}_{6-x}\text{W}_x\text{O}_{24}\text{H}_6](\text{NH}_4)_4 \cdot 5\text{H}_2\text{O}$ ($x=0, 2, 3, 4, 6$) heteropolyoxometallates. Thermal analysis of the precursors, X-ray diffraction and Raman spectroscopy on the mixed oxides were performed. X-Ray powder patterns, collected at the end of the thermal treatment, revealed that the final products are NiMoO_4 and MoO_3 for the $x=0$ composition, whereas for tungsten-containing materials the final products are $\text{Mo}_{1-x}\text{W}_x\text{O}_3$ solid solutions, NiWO_4 and WO_3 , depending on the Mo/W atomic ratio. Raman spectra have confirmed the XRPD analysis, revealing the presence of a stable WO_3 -type phase at high molybdenum contents and a high structural stability of $\text{Mo}_{1-x}\text{W}_x\text{O}_3$ solid solutions.

Heteropolyoxometallates are polymeric species formed by the condensation of more than two oxoanions. Anderson-type heteropolyanions, with the general formula $[\text{XM}_6\text{O}_{24}\text{H}_6]^{n-}$, have received great interest because of their potential applications.¹ The mixed molybdotungstonickelates were first described by Matijevic *et al.*² The compounds (in which M is molybdenum or tungsten and X is a transition-metal atom such as cobalt or nickel) can be used as catalysts directly as bulk materials,³⁻⁵ or deposited on different supports.⁶ Moreover, they form readily, under mild thermal treatment, highly dispersed bi- or tri-metallic oxides (XO/MoO_3 , XO/WO_3 , $\text{XO}/\text{Mo}_{1-x}\text{W}_x\text{O}_3$), metal molybdates or tungstates (XMoO_4 , XWO_4), which are well known catalysts (supported or unsupported on alumina) for industrial oxidation and hydrodesulfurization (HDS) processes.⁷

Structurally, the $[\text{XM}_6\text{O}_{24}\text{H}_6]^{n-}$ anion is made up of a compact package of six MoO_6 octahedra which surround one XO_6 polyhedron in a planar hexagonal configuration.⁸ There are three types of M–O bonds: M–O terminal bonds, M–O(H)–X and M–O–M bridge bonds. A monovalent cation (NH_4^+ , Na^+ , *etc.*) is coordinated by oxygen atoms from the heteropolyanion and some hydration water molecules. Anderson phases are able to lose the hydration water without the destruction of the heteropolyanion structure.

The aim of this work is to complete a previous study on the preparation and characterization of molybdotungstonickelate Anderson-type compounds⁹ examining, by X-ray diffraction and Raman spectroscopy, the structural properties of nickel–molybdenum–tungsten oxides obtained after thermal decomposition of the Anderson phases. In particular, our interest is directed towards the $\text{Mo}_{1-x}\text{W}_x\text{O}_3$ solid solutions which are formed when the Mo–W Anderson phases decompose. The $\text{Mo}_{1-x}\text{W}_x\text{O}_3$ system has been widely studied,^{10,11} and is characteristic because both end members reveal octahedral environments of the metals but different octahedral networks.

Experimental

$[\text{NiMo}_{6-x}\text{W}_x\text{O}_{24}\text{H}_6](\text{NH}_4)_4 \cdot 5\text{H}_2\text{O}$ ($x=0, 2, 3, 4, 6$) were prepared by dropwise addition of nickel sulfate into boiling solutions containing appropriate amounts of $(\text{NH}_4)_4\text{Mo}_7\text{O}_{24} \cdot 4\text{H}_2\text{O}$ and $\text{Na}_2\text{WO}_4 \cdot 2\text{H}_2\text{O}$. Details of the sample characterizations performed by X-ray powder diffraction (XRPD), diffuse reflectance spectroscopy (DRS), magnetic suscep-

tibility and X-ray photoelectron spectroscopy (XPS) are given in ref. 9.

Thermal analysis was performed under air with a Stanton Redcroft STA 781 simultaneous TG–DTG–DTA apparatus (Pt crucibles, Pt–Pt/Rh thermocouples). The heating rate was 5 K min^{-1} from 293 to 873 K for all the samples.

XRPD patterns were obtained for the powders obtained at the end of the thermal treatment by a Philips Debye-Scherrer camera (114.6 mm i.d.) with the asymmetric Straumanis film mounting method. Phase analysis was carried out with Cu-K α (nickel-filtered) radiation. Reflections in the region $2\theta=10\text{--}60^\circ$ were read by means of a Norelco measuring device with an accuracy of $\pm 0.005 \text{ cm}$.

Raman spectra were collected at room temperature by a Spex-Ramalog 1403 double monochromator spectrometer,

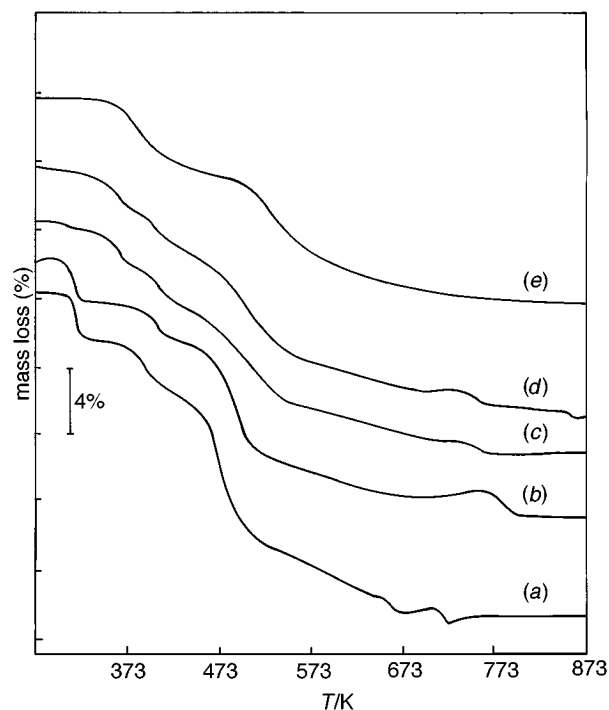


Fig. 1 Thermogravimetry patterns of $[\text{NiMo}_{6-x}\text{W}_x\text{O}_{24}\text{H}_6](\text{NH}_4)_4 \cdot 5\text{H}_2\text{O}$ Anderson phases. (a) $x=0$; (b) $x=2$; (c) $x=3$; (d) $x=4$; (e) $x=6$.

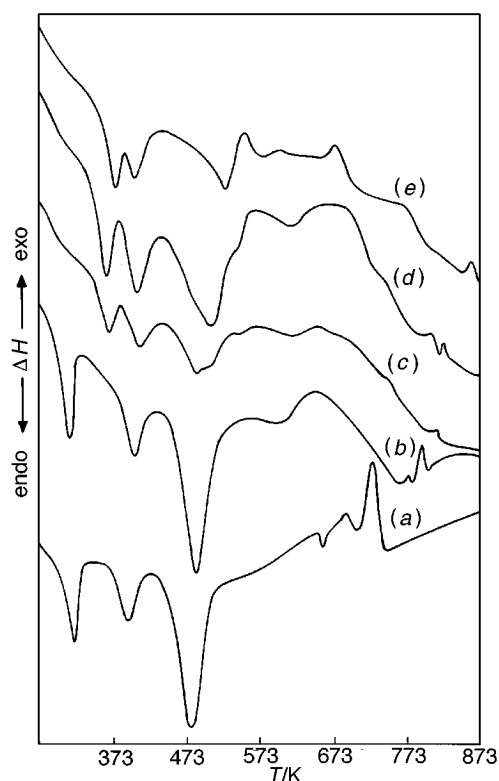


Fig. 2 Differential thermal analysis patterns of $[\text{NiMo}_{6-x}\text{W}_x\text{O}_{24}\text{H}_6](\text{NH}_4)_4 \cdot 5\text{H}_2\text{O}$ Anderson phases. (a) $x=0$; (b) $x=2$; (c) $x=3$; (d) $x=4$; (e) $x=6$.

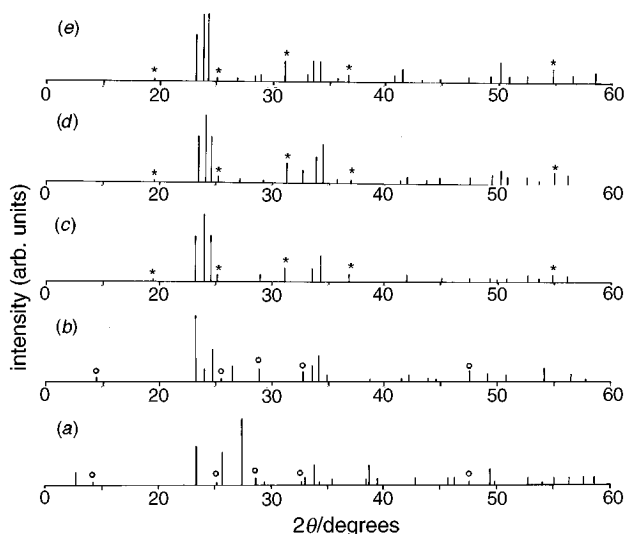


Fig. 3 X-Ray powder diffraction patterns of Anderson phases after thermal treatment at 873 K. (a) $x=0$; (b) $x=2$; (c) $x=3$; (d) $x=4$; (e) $x=6$. \circ , NiMoO_4 ; \times , NiWO_4 .

equipped with a SCAMP data processor. The 514.4 nm line of an Ar ion laser was used for excitation.

Results and Discussion

The thermal analyses performed on the $[\text{NiMo}_{6-x}\text{W}_x\text{O}_{24}\text{H}_6](\text{NH}_4)_4 \cdot 5\text{H}_2\text{O}$ ($x=0, 2, 3, 4, 6$) materials confirm the results given by La Ginestra *et al.*, who showed that the decomposition of $[\text{XMo}_6\text{O}_{24}\text{H}_6](\text{NH}_4)_4 \cdot 5\text{H}_2\text{O}$ materials ($X = \text{Mn, Co, Ni, Cu, Zn}$) occurs in many steps.¹²

Fig. 1 shows the thermogravimetry patterns of all the samples. The mass decrease observed for the molybdenum-containing sample [Fig. 1(a)] below 443 K is due to the loss

of water of hydration, those between 443 and 723 to the elimination of both constitutional water (from the six OH groups bound to nickel) and ammonia. With increasing tungsten content [Fig. 1(b)–(e)] the different mass loss steps become smoother and shifted to higher temperatures. The latter observation is more visible in the DTA patterns reported in Fig. 2, where a delay of about 50 K with respect to the molybdenum compound ($x=0$) is detected for the tungsten sample ($x=6$) in the endothermic peak around 500 K and which corresponds to the loss of both constitutional water and ammonia. Since the three constitutional water molecules must be considered as fundamental in preserving the Anderson-type structure of the samples, the delay in their elimination gives evidence of the higher structural stability of tungsten-containing heteropolyanions with respect to the molybdenum ones.

The two exothermic peaks with maxima at 693 and 723 K in the molybdenum-containing sample ($x=0$) relative to the formation of NiMoO_4 and MoO_3 are also shifted to higher temperatures with increasing tungsten content, indicating a greater structural stability of tungsten-containing oxides, namely Mo–W mixed oxides and NiWO_4 .

The XRPD patterns, collected on the samples obtained at the end of the thermal analysis, are shown in Fig. 3 where the 2θ values and intensities of the observed reflections are reported. The X-ray lines for the nickel molybdate and tungstate minority phases are indicated.

Phase analysis of the $x=0$ compound reveals almost exclusively the presence of orthorhombic MoO_3^{13a} and a small amount of NiMoO_4^{13b} . Patterns of the $x=2, 3$ and 4 compounds show no trace of MoO_3 and reveal the presence of $\text{Mo}_{1-x}\text{W}_x\text{O}_3$ solid-solution phases, namely those reported in the literature as $\text{Mo}_{0.6}\text{W}_{0.4}\text{O}_3$ (θ phase, orthorhombic symmetry)^{13c} and as $\text{Mo}_{0.47}\text{W}_{0.53}\text{O}_3$ (ξ phase, monoclinic symmetry).^{13d} In addition, the pattern of the $x=2$ compound still reveals the presence of NiMoO_4 , while in the $x=3$ and 4 samples NiWO_4^{13f} is formed. Finally, in the $x=6$ compound the triclinic form of WO_3^{13e} and NiWO_4 are the phases present. As reported previously,¹⁰ it may then be derived that a decrease of symmetry (from orthorhombic to triclinic) occurs also in our Mo–W mixed oxide samples with increasing tungsten content. The absence of the MoO_3 phase also at high Mo/W atomic ratio (sample with $x=4$) also reveals that in the mixed Mo–W oxide system it is molybdenum that prefers to enter the WO_3 structure rather than tungsten in the MoO_3 lattice.

Regarding Raman spectroscopy it may be recalled that, in the condensed phases we have investigated, Mo^{VI} and W^{VI} are in octahedral coordination.¹⁴ Thus they show patterns more complex than those observed for the same species in simple oxide systems, as those obtained by thermal treatment of the original Anderson phase. In fact, for tetrahedral or octahedral symmetry the internal modes associated to the W–O or Mo–O stretchings are located in characteristic regions of the spectra.^{15–17} So, for molybdate ion these Raman lines are located in the 800–870 cm^{-1} region while some lines observed at higher wavenumbers (at about 950 cm^{-1}) can be assigned to Mo–O terminal bonds.¹⁸

Fig. 4 shows Raman spectra of all the samples heated to 873 K. The $x=0$ sample [Fig. 4(a)] reveals the typical spectrum of MoO_3 with the three most intense lines at 665, 819 and 994 cm^{-1} .¹⁰ Some additional weak bands at 881, 898, 916, 937 and 959 cm^{-1} are attributed to tetrahedral MoO_4 species of NiMoO_4 .¹⁹

On the other hand, the $x=6$ sample [Fig. 4(e)] shows the typical Raman spectrum of WO_3 with the strongest lines at 715 and 807 cm^{-1} .¹⁰ Some additional weak bands corresponding to NiWO_4 can be observed in the region around 900 cm^{-1} .¹⁹

The Raman spectrum of the most dilute tungsten mixed oxide [$x=2$, Fig. 4(b)] compared to that of the $x=0$ sample,

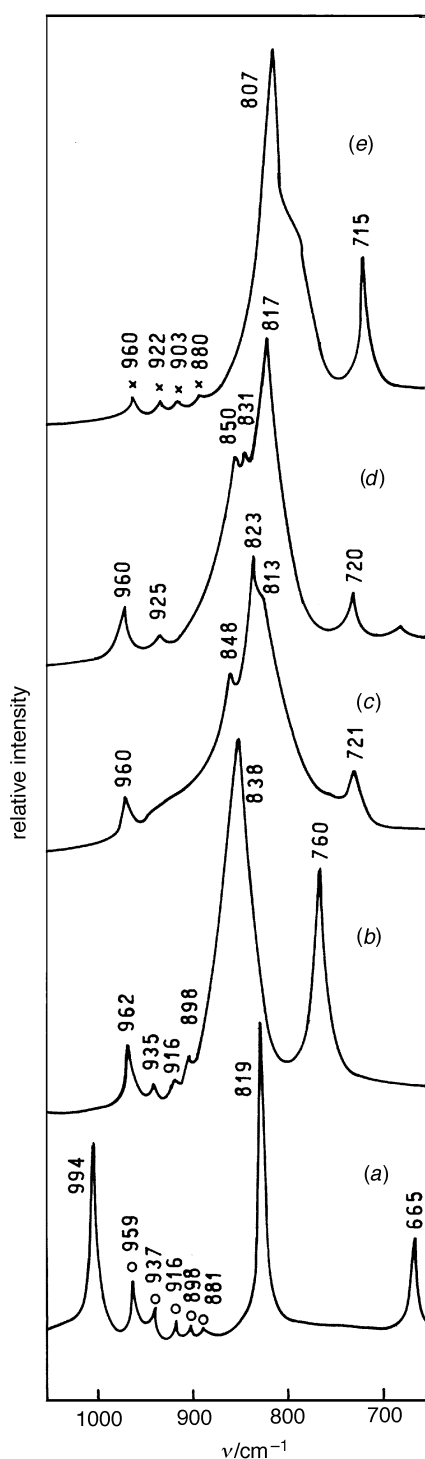


Fig. 4 Raman spectra of Anderson phases after thermal treatment at 873 K. (a) $x=0$; (b) $x=2$; (c) $x=3$; (d) $x=4$; (e) $x=6$. \circ , NiMoO_4 ; \times , NiWO_4 .

shows a shift towards higher frequency for the strongest line (from 819 to 838 cm^{-1}) as well as the disappearance of the lines at 665 and 994 cm^{-1} . This is related to the formation of the $\text{Mo}_{1-x}\text{W}_x\text{O}_3$ solid solution which presents a WO_3 -type structure, also at high molybdenum content.

With increasing tungsten content [samples with $x=3, 4$, Fig. 4(c), (d)] the spectra resemble more and more that of the WO_3 phase [$x=6$, Fig. 4(e)]. However, the most intense Raman line at ca. 800 cm^{-1} is broad and split. This is probably due to a decrease of symmetry caused by the presence of more than one type of atom in the lattice.

In the spectrum of the $x=2$ sample [Fig. 4(b)] the weak lines due to NiMoO_4 are still clearly visible, whereas only for the sample with $x=6$ [Fig. 4(e)] can the weak bands corresponding to NiWO_4 be observed in the region around 900 cm^{-1} .

Conclusions

XRPD and Raman analyses on the mixed oxides obtained by thermal decomposition at 873 K of $[\text{NiMo}_{6-x}\text{W}_x\text{O}_{24}\text{H}_6](\text{NH}_4)_4 \cdot 5\text{H}_2\text{O}$ ($x=0, 2, 3, 4, 6$), Anderson-type heteropolymetallates have revealed that: (i) the products are NiMoO_4 and MoO_3 for the $x=0$ compound, whereas for tungsten-containing materials the final products are $\text{Mo}_{1-x}\text{W}_x\text{O}_3$ solid solutions, NiWO_4 and WO_3 , depending on the Mo/W content; (ii) the presence of a stable WO_3 -type phase, also at high molybdenum content, indicates that Mo^{VI} ions enter the WO_3 lattice preferably rather than W^{VI} into the MoO_3 one.

References

- 1 M. T. Pope, *Heteropoly and Isopolyoxometallates*, Springer, Berlin, 1983.
- 2 E. Matijevic, M. Kerker, H. Beyer and F. Theubert, *Inorg. Chem.*, 1963, **2**, 581.
- 3 M. T. Pope, *Prog. Inorg. Chem.*, 1991, **39**, 181.
- 4 M. T. Pope and A. Muller, *Angew. Chem., Int. Ed. Engl.*, 1991, **30**, 34.
- 5 M. Misono, *Catal. Rev. Sci., Eng.*, 1987, **29**, 269.
- 6 M. Fournier, R. Thouvenot and C. Rocchiccioli-Deltcheff, *J. Chem. Soc., Faraday Trans.*, 1991, **87**, 349.
- 7 M. Fournier, C. Louis, M. Che, P. Chaquin and D. Masure, *J. Catal.*, 1989, **119**, 400.
- 8 H. Kondo, A. Kobayashi and Y. Sasaki, *Acta Crystallogr., Sect. B*, 1980, **36**, 661.
- 9 P. Porta, G. Minelli, G. Moretti, I. Pettiti, L. I. Botto and H. J. Garcia, *J. Mater. Chem.*, 1994, **4**, 541.
- 10 E. Salje, R. Gehlig and K. Viswanathan, *J. Solid State Chem.*, 1978, **25**, 239, and refs. therein.
- 11 F. Harb, B. Gérard and M. Figlarz, *C. R. Acad. Sci. Paris*, 1986, **9**, 303, and refs. therein.
- 12 A. La Ginestra, F. Giannetta and P. Fiorucci, *Gazz. Chim. Ital.*, 1968, **98**, 1197.
- 13 X-Ray Powder Data Files: (a) 35–609 for MoO_3 , (b) 33–948 for NiMoO_4 , (c) 32–1391 for $\text{Mo}_{1-x}\text{W}_x\text{O}_3$ ($x=0.40$), (d) 32–1392 for $\text{Mo}_{1-x}\text{W}_x\text{O}_3$ ($x=0.53$), (e) 32–1395 for WO_3 , (f) 15–755 for NiWO_4 .
- 14 J. L. Botto, A. C. Garcia and H. J. Thomas, *J. Phys. Chem. Solids*, 1992, **53**, 1075.
- 15 K. Nakamoto, in *Infrared and Raman Spectra of Inorganic and Coordination Compounds*, John Wiley, New York, 1986, pp. 138, 155.
- 16 S. D. Ross, in *Inorganic Infrared and Raman Spectra*, McGraw Hill, London, 1972, p. 204.
- 17 G. M. Clark and W. P. Doyle, *Spectrochim. Acta*, 1966, **22**, 1441.
- 18 F. D. Hardcastle and J. E. Wachs, *J. Raman Spectrosc.*, 1990, **21**, 603.
- 19 S. Sheik Saleem and G. Aruldas, *Polyhedron*, 1982, **1**, 331.

Paper 6/04875G; Received 11th July, 1996